2007 IEEE International Conference on
Robotics and Automation
Roma, Italy, 10-14 April 2007

Design and Optimization of a Biologically Inspired Flapping Mechanism for Flapping Wing Micro Air Vehicles

Zaeem A. Khan, Graduate Student
Department of Mechanical Engineering
University of Delaware, Newark, DE, 19716
zaeem@udel.edu

Sunil K. Agrawal. PhD., Professor
Department of Mechanical Engineering
University of Delaware, Newark, DE, 19716
agrawal@udel.edu

***Abstract*— In this paper, we investigate design and performance of a flapping mechanism which generates flapping motion through resonant excitation similar to flight apparatus of insects. The desired flapping motion is based on optimum aerodynamic efficiency. The mechanism is driven by a conventional motor and gearbox. The rotary motion is converted into oscilltory excitation through a four-bar linkage. This study explores the optimal design parameters of this mechanism for peak performance.**

I. Introduction

Micro Air vehicles (MAVs) represent an emerging class of aerial vehicles that can be used as surveillance platforms for numerous applications. The extremely agile and maneuverable flight characteristics exhibited by biological species such as hummingbirds and insects make them a strong candidate for MAV design. However, the design of MAV that can achieve this performance is still a lofty goal. Even the design of efficient flapping mechanisms to generate flapping motion is a challenging problem. There have been attempts to generate complex insect-like wing motion using rigid mechanisms [4], [5],[6]. These mechanisms generate the desired kinematics at the cost of complexity and weight. However, the wing motion of natural flyers is a result of resonant excitation of their aeroelastically tailored wing structure. Their flapping apparatus is a non-linear oscillator. There have been attempts to mimic this feature [9], [10]. However, these mechanisms utilize piezoelectric actuators which require bulky power source. Furthermore, these studies assume linear spring stiffness and aerodynamic damping. Other studies have tried to investigate the use of springs for reducing the peak torques and power during the flapping cycle [3], [8].

In this paper, we present the design and optimization methodology of a resonant flapping mechanism motivated from study of insect wing motion. This mechanism while benefiting from the resonance excitation has the added simplification in that it can be driven by a simple four-bar mechanism through a conventional micro DC motor and gearbox. The design involves study of aerodynamics, dynamics of the oscillator and power source. The design is based on optimum performance of all three areas, when integrated. Furthermore, aerodynamic damping and non-linear spring is used in the analysis.

A. Motivation For Design

Biological wings are elastic structures which deform under aerodynamic loads. The wing structure is composed of a thick and heavy leading edge and light wing surface made up of thin viens embedded in membrane. The complex wing motion can be decomposed into flapping and rotation as shown in Fig. 1. The flapping motion is brought about by the thorax muscles and involves transverse elastic bending near the wing base as shown in Fig. 1. The transverse bending amplifies the flapping amplitude when excited by the thorax [2]. Rotation involves continuous twisting of the wing about the torsion axis parallel to the leading edge from the base to the tip. The torsion could be passive or active. Passive torsion is imposed by the aerodynamic and inertial loads near the end of the stroke and serves to maintain optimum angle of attack distribution during the entire flap cycle. The extent of torsion depends on the stiffness distribution of the wing. Active torsion is applied at the base by the muscles of the thorax for flight control [7].

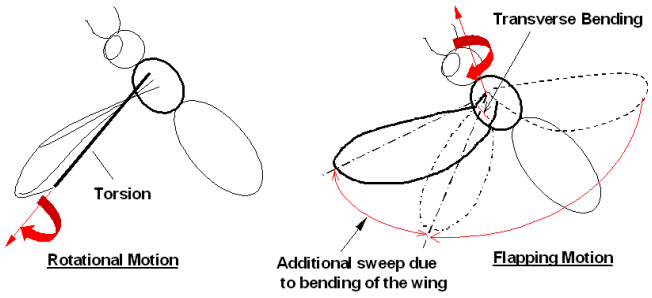

Fig. 1. **Figure shows the details of insect wing motion which includes elastic deformations of the wings.**

Motivated from this study, we propose a flapping mechanism which utilizes a simplified analog of the complex biological wing. The wing comprises of a stiff circular leading edge spar attached to a light wing surface as shown in Fig. 2A. The leading edge spar rotates freely in a circular tube called the wing holder which serves as a bearing. A torsion spring is attached between the spar and the wing holder Fig. 2B. This is the rotational motion given by ψ. The wing holder is attached to a driving lever through another torsion spring as shown in Fig. 2C. This is the flapping motion denoted by θ. The motion of the driving lever is given by ϕ. Note that the flapping motion is generated through excitation from the driving lever, while the rotational motion

is passive. This is basically a coupled oscillator system. Further details in Fig. 2 are explained in the following sections.

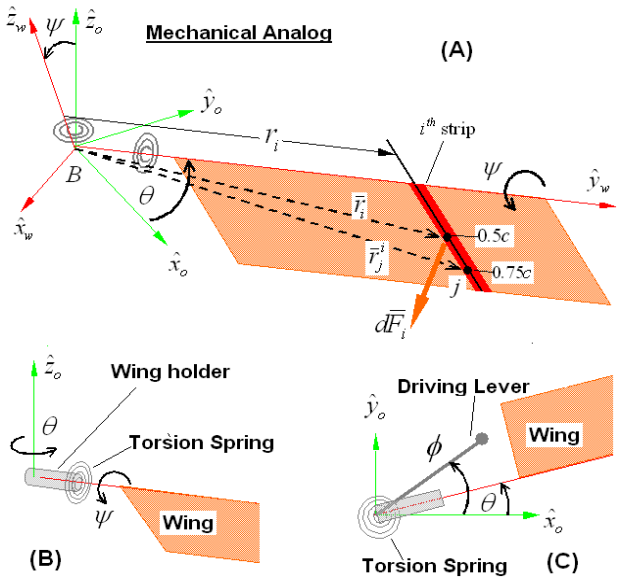

Fig. 2. **Figure shows the details of the biologically inspired wing design to generate insect-like flapping and rotational motions when excited through the driving lever.**

B. Design Optimization Procedure

The design of an efficient flapping mechanism not only involves the dynamics of the oscillator but also the aerdynamics and actuator dynamics. The complete flapping mechanism is a combination of these three components. Therefore, the design should involve the optimum performance of all three components when integrated. The actuator (thorax muscles in the case of insects) resonates the coupled wing oscillator system to generate lift. The force and energy flow through the system is from the actuator to the surrounding air. The optimization procedure that is adopted in this paper optimizes the energy flow through the three components. The procedure is explained in Fig. 3. The design goal is to generate enough lift 'L' to support the weight 'mg' of the FWMAV from the available actuator output power 'P_o'. The optimum operating point of each component may not match with the other, therefore, the scheme is iterative.

The outline of the rest of the paper is as follows. In Section II, we discuss the aerodynamic efficiency in terms of lift and required power and set the kinematic requirements for the flapping mechanism. In Section III, we discuss the oscillator dynamics and derive the equations of motion. In Section IV, we present the actuator dynamics and optimize the performance of the complete mechanism. Finally, in Section V, we present conclusions.

II. Aerodynamic Efficiency

A. Momentum Theory

A first order relationship between lift and power can be derived using momentum theory without actually having to

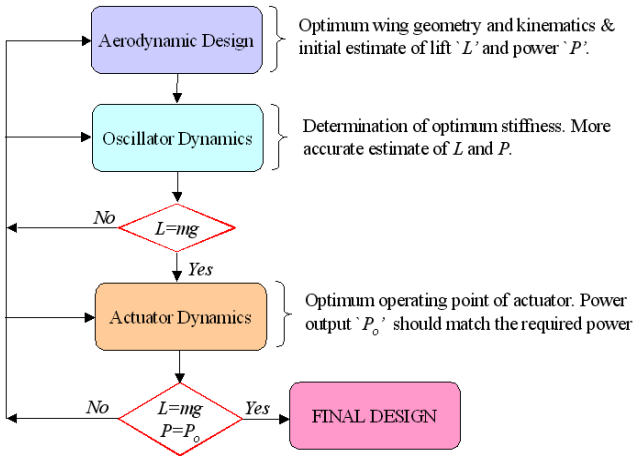

Fig. 3. **Figure shows the three components of the flapping mechanism design and the optimization scheme based on the optimum energetic performance of these components.**

consider the details of the flow environment [11]. The main body of flow around the FWMAV is enclosed in a control volume 'CV' having a surface area S and let $\hat{d}S$ be a unit normal area vector pointing out of CV as shown in Fig. 4A. The CV is divided into three cross sections. cross section '0' denotes the plane far upstream of the stroke plane where the velocity $v_o = 0$. Cross section 1 is just below the stroke plane and cross section ∞ is well below the stroke plane. The velocity induced by the flapping wings at the stroke plane is denoted by v_s whereas at plane ∞ it is v_∞. Let A_o, $A_s \approx A_1$ and A_∞ be the cross sectional areas at these planes, as shown shaded in Fig 4A. The stroke plane cross-sectional area is given by $A_s = 2\Phi R^2$.

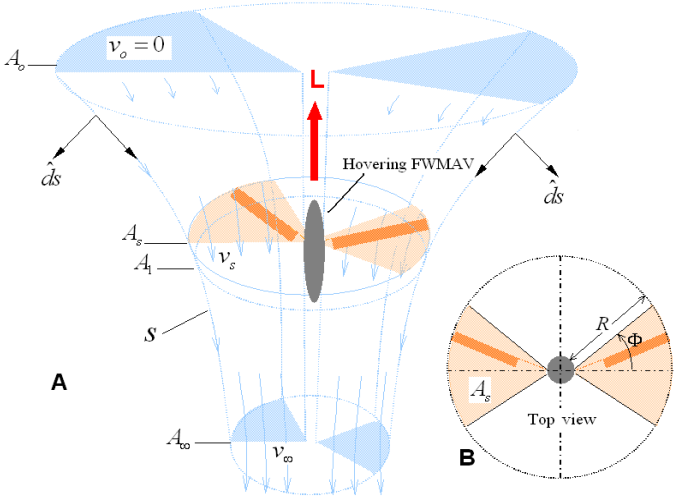

Fig. 4. **(A) The control volume around FWMAV in hovering flight. (B) Top view showing the cross-section of the control volume at the stroke plane.**

Based on the assumptions of momentum theory, the following principles of mass conservation, momentum and

energy apply on this CV

$$\int_S \rho\bar{v}.\hat{dS} = 0, \quad L = \int_S (\rho\bar{v}.\hat{dS})\bar{v}, \quad P = \frac{1}{2}\int_S (\rho\bar{v}.\hat{dS})|\bar{v}|^2, \quad (1)$$

where $\bar{v}$ is the local flow velocity vector, L is the lift force vector which is equal and opposite to the net force imparted on the fluid by the flapping wings and P is the work done per unit time by the flapping wings equal to the gain in kinetic energy of the fluid per unit time. Application of the above principles gives

$$\dot{m} = \int_\infty \rho\bar{v}.\hat{dS} = \int_1 \rho\bar{v}.\hat{dS} = \rho A_\infty v_\infty = \rho A_s v_s \quad (2)$$

$$L = \rho(\int_\infty (\bar{v}.\hat{dS})\bar{v} - \int_o (\bar{v}.\hat{dS})\bar{v}) = \dot{m}v_\infty \quad (3)$$

$$Lv_s = \frac{\rho}{2}(\int_\infty (\bar{v}.\hat{dS})|\bar{v}|^2 - \int_o (\bar{v}.\hat{dS})|\bar{v}|^2) = \frac{1}{2}\dot{m}v_\infty^2 \quad (4)$$

From Eq. (3) and (4), we get $v_\infty = 2v_s$. Substituting this value of v_∞ into Eq. (3) and using Eq. (2), we get

$$L = \dot{m}v_\infty = 2\rho A_s v_s^2 = 4\rho\Phi R^2 v_s^2 \quad (5)$$

$$P = Lv_s = 2\rho A_s v_s^3 = 4\rho\Phi R^2 v_s^3 \quad (6)$$

From Eqs (5) and (6), it can be seen that the power required to hover increases with the cube of v_s. The flow velocity at the stroke plane v_s is related to the flapping frequency. Therefore, in order to hover at minimum power, the flapping frequency should be reduced and instead, the stroke amplitude Φ and wing length R should be increased.

B. Optimum angle of attack

The aerodynamic model used to compute the aerodynamic force is given in detail in [1]. The model uses blade element analysis in which the wing is divided into a number of elements or strips along the wing span and the aerodynamic force is computed for each element and then integrated to get the total force. For the purpose of analysis, we attach a co-ordinate system to the wing $(\hat{x}_w, \hat{y}_w, \hat{z}_w)$ as shown in Fig. 2A. The wing motion is given by the co-ordinates (θ, ψ) with respect to the fixed frame $(\hat{x}_o, \hat{y}_o, \hat{z}_o)$. As shown in Fig. 2A, the aerodynamic force vector at the i^{th} strip of the wing acts normal to the chord at the mid-chord location. Its magnitude is given by

$$|d\bar{F}_i| = -C_1(\alpha_i)\frac{\rho}{2}\,|\bar{V}_i|^2 c\; dr\; sign(V_{ix}), \quad (7)$$

where c is the chord length, dr is the width of the strip, $\bar{V}_i$ is the flow velocity vector of a point 'j' on the i^th strip located at 75% chord length from leading edge as shown in Fig. 2A. This is given by

$$|\bar{V}_i|^2 = V_{ix}^2 + V_{iz}^2 = (\frac{3c}{4}\dot{\psi} + r_i\dot{\theta}\cos\psi)^2 + (r_i\dot{\theta}\sin\psi)^2 \quad (8)$$

Where the V_{iy} component is set to zero since it does not contribute to the aerodynamic force. The aerodynamic coefficient C_1, determined from experiments [1], is approximated as a function of angle of attack α_i. These are given by

$$C_1 = \frac{7}{\pi}|\alpha_i| \quad , \quad \alpha_i = \arctan\left(\frac{V_{ix}}{V_{iz}}\right). \quad (9)$$

During flapping phase, the wing is held at a constant angle of attack and rotation occurs mainly during the end of each stroke. In order to study the generation of aerodynamic force during the flapping phase, we assume that $\dot{\psi} = 0$ and $\psi =$ constant. Based on this assumption, Eq. (7) can be simplified as follows

$$|d\bar{F}_i| = \frac{7}{\pi}(\frac{\pi}{2} - \psi)\frac{\rho}{2}c\; dr\; r_i^2\dot{\theta}^2, \quad (10)$$

where $\alpha_i = \alpha = \frac{\pi}{2} - \psi$ and remains constant for all the wing strips. Based on Eq. (10), the magnitude of lift and drag of the i^{th} wing strip during the flapping phase are given by

$$dL_i = |d\bar{F}_i|\sin\psi \quad , \quad dD_i = |d\bar{F}_i|\cos\psi. \quad (11)$$

The plot of dL_i and dD_i as a function of α is given in Fig. 5. This plot shows that lift to drag ratio is maximum when $20^o \leq \alpha \leq 30^o$ deg. Furthermore, to achieve maximum lift at maximum L/D ratio, the optimum operating angle of attack is roughly $\alpha^* = 30^o$ deg which implies optimal rotation angle of $\psi^* = \pm 60^o$ deg which is used in subsequent analysis.

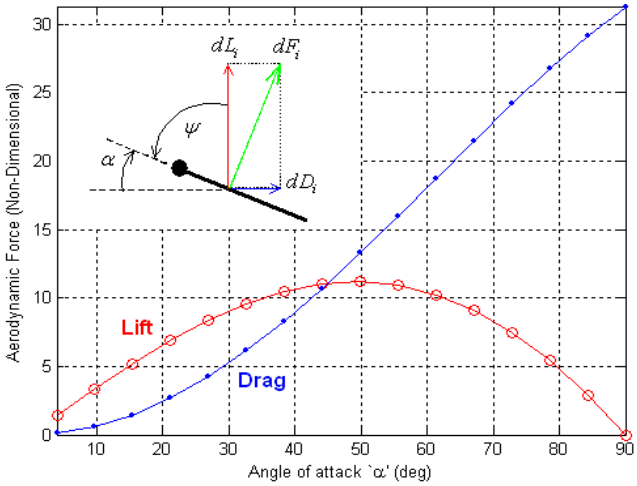

Fig. 5. **Figure showing a plot of section lift to drag as a function of angle of attack α.**

III. Oscillator Dynamics

In Section II, it was shown that to achieve maximum aerodynamic efficiency, the flapping amplitude should be maximized and the optimal rotation ψ^* should be maintained during the flapping phase. These are two important requirements for the flapping mechanism. In this section, the dynamics of the coupled oscillator is investigated to see how these requirements can be met.

A. Dynamic Model

The coupled oscillator is a 2 DOF system, i.e, $\Theta = (\theta, \psi)^T$.The kinetic energy is given by

$$T = \frac{1}{2}\omega^T I_B \omega + \frac{1}{2} J_h \dot{\theta}^2 \tag{12}$$

where J_h is the inertia of the wing holder and I_B is the inertia matrix of the wing in the wing frame and about the wing base B. It is given by

$$I_B = \begin{pmatrix} J_x & 0 & 0 \\ 0 & J_y & J_{yz} \\ 0 & J_{yz} & J_z \end{pmatrix}, \tag{13}$$

where J_{yz} is non-zero due to the asymmetry in the $(\hat{y}_w, \hat{z}_w)$ plane. The potential energy is given by

$$\begin{aligned} V = -M_w g z_w \cos\psi + \frac{1}{2}K_{f1}\delta^2 + \frac{1}{4}K_{f2}\delta^4 \\ + \frac{1}{2}K_{r1}\psi^2 + \frac{1}{4}K_{r2}\psi^4 + \frac{1}{2}K_{r3}\psi^2 \end{aligned} \tag{14}$$

where M_w is the mass of the wing, $z_w = c/2$ is the location of center of mass of the wing, $\delta = \phi - \theta$ is the flapping spring deflection where $\phi = \Phi_o \sin\omega t$ is the motion of the driving lever, ω is the driving frequency and Φ_o is the driving amplitude, K_{f1}, K_{f2} are the parameters of the non-linear flapping spring and K_{r1}, K_{r2} and K_{r3} are parameters of the non-linear rotational spring. The additional parameter K_{r3} is a discontinuous function of ψ and its significance is explained later. The virtual work can be written as

$$\delta W = M_B.\delta\Theta - c_r\dot{\psi}.\delta\psi, \tag{15}$$

where c_r is the coefficient of friction between the wing spar and the wing holder, $\delta\Theta$ is the variation of angular velocity of the wing. M_B is the resultant aerodynamic moment at the wing base 'B' computed as a summation of aerodynamic moments from all the wing elements, given by

$$M_B = \sum_{i=1}^{N} \bar{r}_i \times d\bar{F}_i = -\sum_{i=1}^{N} (\frac{c}{2}\hat{y}_w + r_i\hat{z}_w)|d\bar{F}_i|, \tag{16}$$

where $\bar{r}_i = r_i\ \hat{y}_w - \frac{c}{2}\hat{z}_w$ is the vector from the base of the wing to the mid-chord location of aerodynamic force at the i^{th} strip. The equation of motion is given by

$$M(\Theta)\ddot{\Theta} + C(\Theta, \dot{\Theta}) + G(\Theta) = Q_\Theta \tag{17}$$

where $M(\Theta)$ is the inertia matrix given by

$$M(\Theta) = \begin{pmatrix} \sin^2\psi J_x + \cos^2\psi J_z + J_h & \cos\psi J_{yz} \\ \cos\psi J_{yz} & J_y \end{pmatrix}, \tag{18}$$

$C(\Theta, \dot{\Theta})$ is the centrifugal term given by

$$C(\Theta, \dot{\Theta}) = \begin{pmatrix} \sin 2\psi(J_x - J_z)\dot{\theta}\dot{\psi} - \sin\psi J_{yz}\dot{\psi}^2 \\ \frac{1}{2}\sin 2\psi(J_x - J_z)\dot{\theta}^2 \end{pmatrix}. \tag{19}$$

The potential term $G(\Theta)$ is given by

$$G(\Theta, \dot{\Theta}) = \begin{pmatrix} K_{f1}(\phi - \theta) + K_{f2}(\phi - \theta)^3 \\ M_w g z_w \sin\psi + K_{r1}\psi + K_{r2}\psi^3 + K_{r3}\psi \end{pmatrix}. \tag{20}$$

From Eq. (15) and (16), the generalized force vector can be written as

$$Q_\Theta = \begin{pmatrix} -\cos\psi \sum_{i=1}^{N} r_i |d\bar{F}_i| \\ -\frac{c}{2}\sum_{i=1}^{N} |d\bar{F}_i| - c_r\dot{\psi} \end{pmatrix}. \tag{21}$$

The dynamic equation, Eq. (17) along with the aerodynamic model given by Eq. (7) constitutes the complete model of the system.

B. Wing Rotation

As outlined in Section II, the maximum lift to drag ratio is obtained when $\psi^* = \pm 60^o$ is maintained during the entire flapping cycle except during rotational phase. This can be achieved by designing the rotational spring in such a way that the rotational stiffness increases sharply as ψ approaches ψ^*. Physically this implies a lock placed on wing rotation so that $\psi \leq \psi^*$. Mathematically this is achieved by invoking K_{r3} as follows

$$K_{r3} = \begin{cases} 0, & \text{if } \psi < \psi^* \\ K_{r3}, & \text{if } \psi \geq \psi^* \end{cases} \tag{22}$$

In order for the lock to take effect $K_{r3} \gg K_{r1} = K_{r2}$. The steady state simulation results including the lift generated by the wing are presented in Fig. 6. The results show that the rotational spring tries to maintain $\psi^* = \pm 60^o$ during the flapping phase as flapping angle θ varies between $\pm 90^o$. As θ approaches one of the extreme positions, the wing rotates and settles at ψ^*. The sharp peaks of lift coinciding with wing rotation are due to rotational lift [1].

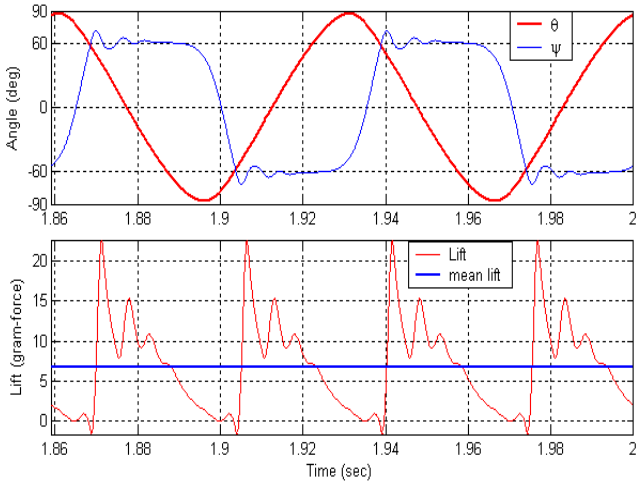

Fig. 6. **Figure showing the simulation results of the coupled oscillator system which includes wing rotational degree of freedom.**

The important quantities of interest to us are the steady state values of flapping amplitude $\Phi = |\theta_{max}|$ and the average lift L and input power P over one cycle given by

$$L = \frac{1}{T}\int_o^T |d\bar{F}_i| \sin\psi dt \tag{23}$$

$$P = \frac{1}{T}\int_o^T [K_{f1}(\phi-\theta) + K_{f2}(\phi-\theta)^3]\ \dot{\phi}\ dt \tag{24}$$

where L is obtained by summing Eq. (11) and integrating over one cyle. The expression for $|d\bar{F}_i|$ is substituted from Eq. (7). The steady-state values of L and P are obtained by numerically intergrating Eq. (17).

IV. Actuator Dynamics

The actuator consists of motor, gear box and a mechanism which converts the rotary motion into oscillatory motion. As shown in Fig. 7, the mechanism consists of two independent four-bars driven by a common crank 'l_1'. The rocker 'l_3' is now the driving link. The wing holder 'l_4' is connected to the rocker through the torsion spring. There is another torsion spring between the wing holder and the wing itself.

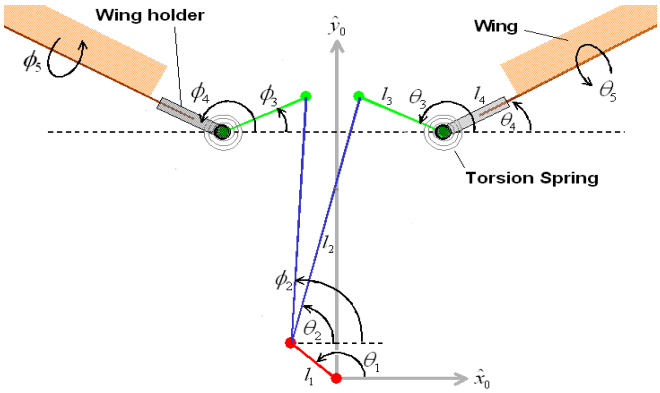

Fig. 7. **Details of the double fourbar mechanism. The left and right rockers now become the driving link**

The link lengths of the mechanism can be optimized to achieve a sinusoidal motion with a driving amplitude of $\Phi_o = 30^0$ with sufficient symmetry between the left and right rocker motions as shown in Fig. 8. The optimization was performed using $fmincon()$ function in MATLAB.

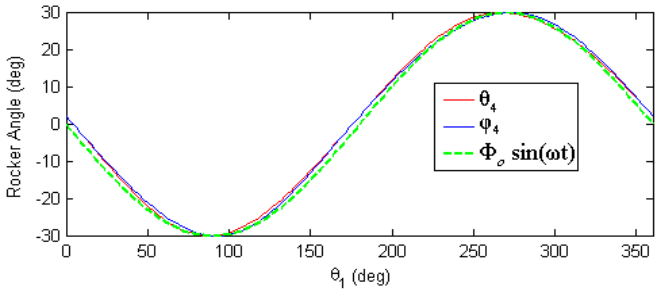

Fig. 8. **Optimization result of the double four-bar mechanism showing the sinosoidal motion of the left and right rocker angles with sufficient symmetry.**

A micro DC motor known as KP-00 was selected for the actuator. This motor weighs a mere 5 grams and can generate upto 1.6 Watts of power. A two stage gear box is used between the motor and the crank shaft. The dynamics of the transmission in terms of crank shaft can be written as

$$I_1\ddot{\theta}_1 + B_1\dot{\theta}_1 = n\tau_m - \tau_l \tag{25}$$

where n is the gear ratio, τ_m is the motor torque, τ_l is the load torque which includes load torque of the mechanism and the wings. The load torque from the mechanism can be ignored because of negligible inertia of the links compared to the wings. We also assume that the four-bar mechanism is frictionless. I_1 and B_1 are the inertia and the coefficient of friction of the transmission respectively, given by

$$I_1 = n^2 I_m + n_i^2 I_i + I_s, \tag{26}$$

$$B_1 = n^2 B_m + n_i^2 B_i + B_s. \tag{27}$$

where the letters 'I' and 'B' denote the inertia and friction coefficients and subscripts m, i and s denote the motor, intermediate stage and shaft respectively, n_i is the gear ratio of the intermediate stage. To generate sinusoidal rocker motion, constant crankshaft speed is required. This can be achieved by increasing the inertia I_1, if required by a flywheel. From Eq. (26), it can be seen that the best way to increase I_1 is by increasing the motor inertia J_m, since even a slight increase in inertia will be magnified by the square of the gear ratio. This can be achieved by putting a light weight flywheel on the motor shaft. The motor current and torque τ_m are given by

$$I = \frac{V - nK_b\dot{\theta}_1}{R_m}, \quad \tau_m = K_m I \tag{28}$$

where K_m is the torque constant, K_b is the back emf constant, R_m is the motor resistance and V is the applied voltage. At steady state $\ddot{\theta}_1 = 0$, therefore, using Eqs. (28), Eq. (25) can be written as

$$\tau_l = \frac{nK_mV}{R_m} - \Big(\frac{n^2K_mK_b}{R_m} + B_1\Big)\dot{\theta}_1. \tag{29}$$

The output power P_o, input power P_i and the transmission efficiency η are given by

$$P_o = \tau_l.\dot{\theta}_1, \quad P_i = V.I, \quad \eta = \frac{P_o}{P_i}. \tag{30}$$

The steady state performance of the transmission in terms of the output power and efficiency is given in Fig. 9. The dotted curve shows the case when transmission friction is zero, i.e, $B_i = B_s = 0$. The friction reduces the output power as well as the efficiency of the motor. In Fig. 9, we see two optimum operating points of the transmission, i.e, at peak power P_o^* ($P_o = 1.5$ Watts @ $\dot{\theta}_1 = 9.2$ cycles/sec) and at peak efficiency η^* ($P_o = 0.45$ Watts @ $\dot{\theta}_1 = 14.0$ cycles/sec)

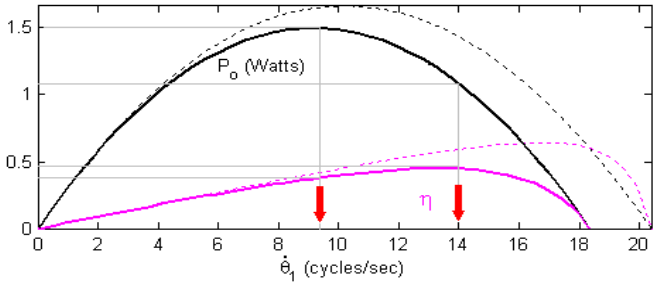

Fig. 9. **Figure shows the steady state performance of the transmission. The supplied voltage is 3.3 volts. The dotted curves refers to the case when $B_i = B_s = 0$. The red arrows indicate optimum operating points.**

as indicated by the arrows. Operating the transmission at peak power generates more power at the cost of faster battery discharge. Maximum power is desirable for hovering and payload carrying capability while peak efficiency is more suitable for longer flight duration. The power required to flap one wing will be half of the above values.

A. Optimized Design

Based on the optimum operating points of the actuator, we perform the design optimization at both P_o^* and η^*. The masses of various components of FWMAV are KP-00 motor (5 gm), gearbox (3 gm), li-poly cell (3.6 gm), control system (5.5 gm), Wings + frame and four-bar mechanism (5.0 gm). This gives a total mass of roughly 22 gm.

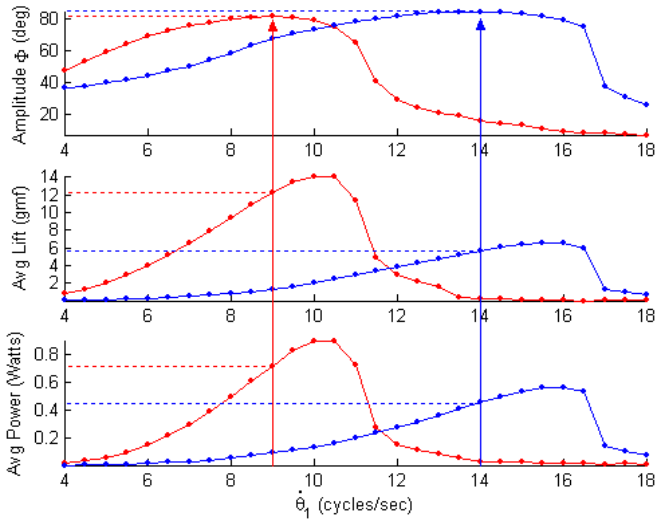

Fig. 10. **Figure shows the steady-state response of one wing at peak efficiency η^* (blue) and peak output power P_o (red).**

Following the optimization procedure of Fig. (3), we get the steady-state response for both operating points given in Fig. (10). The L and P values shown in Fig. (3) are for one wing only. The stiffness and wing geometric and inertia parameters are varied in such a way that the peak amplitude Φ^* occurs at the two optimal operating speeds of the actuator and satisfy $P = P_o$ at these speeds. The peak amplitude is roughly same in both cases as shown by the verticle arrows, however, the difference is in the total average lift L and power P. Optimizing at η^* does not satisfy $L = mg$. Therefore, the system can only be optimized at P_o^* where $L \approx 24$ gmf $> mg$. The optimized wing geometry is roughly 50% larger compared to the η^* case. This is because the wing has to absorb the extra power at a slower flapping speed.

V. CONCLUSIONS AND FUTURE WORKS

In this paper, our attempt was to investigate the design and optimum performance criteria of a biologically inspired resonance based flapping mechanism for FWMAV applications. The mechanism is studied as an integration of three components: aerodynamics, oscillator dynamics and actuator (includes four-bar mechanism and DC motor). The kinematic requirements are determined on the basis of maximum aerodynamic efficiency. Based on these requirements as well as the desired lift and available power, the optimum parameters of the oscillator and wing as well as the optimum operating point of the actuator are determined. The results based on conservative estimate of FWMAV mass seem promising. However, these will be varified by performing the optimization of a real system in future.

VI. ACKNOWLEDGMENTS

The authors gratefully acknowledge the funding of NSF and ARO in support of this work.

REFERENCES

[1] Khan, Z. A., Agrawal, S. K., 2005."Wing force and moment characterization of flapping wings for micro air vehicle application". *American Control conference 2005*.

[2] Khan, Z. A., Agrawal, S. K., 2006."Design of Flapping Mechanisms Based on Transverse Bending Phenomena in Insects". *IEEE International Conference on Robotics and Automation, Orlando, Florida, USA, May. 2006*.

[3] Madangopal, R., Khan, Z. A., Agrawal, S. K., "Biologically inspired design of small flapping wing air vehicles using four-bar mechanisms and quasi-steady aerodynamics". *Journal of Mechanical Design, Vol. 127, No.4, 2005, 809-816*.

[4] Zbikowski, R., Galinski, C., Pedersen, B. C., "Four-Bar Linkage Mechanism for Insect like Flapping Wings in Hover: Concept and an Outline of Its Realization". *Journal of Mechanical Design, Vol. 127, No.4, 2005, 817-824*.

[5] Banala, S. K., Agrawal, S. K., "Design and Optimization of a Mechanism for Out-of-Plane Insect Winglike Motion With Twist". *Journal of Mechanical Design, Vol. 127, No.4, 2005, 841-844*.

[6] McIntosh, S. H., Khan, Z. A., Agrawal, S. K., "Design of a Mechanism for Biaxial Rotation of a Wing for a Hovering Vehicle", *IEEE/ASME TRANSACTIONS ON MECHATRONICS, 2006, VOL. 11, NO. 2.*

[7] Wootton, R. J. 1981," Support and deformability in insect wings". *Journal of Zool, 193:477-68*.

[8] Kurien, K. I., Agrawal, S. K., 2005."An investigation into the use of springs and wing motions to minimize the power expended by a pigeon-sized mechanical bird for steady flight". *ASME International Design Engineering Technical Conferences, IDETC/CIE'2005* .

[9] Raney, L. D., slominski, C. E., 2003."Mechanization and control concepts for biologically inspired micro aerial vehicles". *AIAA 2003-5354, AIAA Guidance, Navigation and Control Conference, Austin, Texas, August 11-14* .

[10] Fearing. R, Chiang. K, Dickinson. M, Pick. D, Sitti. M, and Yan. J ."Transmission mechanism for a micromechanical flying insect". *Proc. of the IEEE International Conference on Robotics and Automation, pp. 1509-1519, San Francisco, CA, USA, Apr. 2000*.

[11] Leishman, G. J, "Principles of Helicopter Aerodynamics". *Cambridge University Press. 2000.*